OPEN ACCESS

KING'S College LONDON

King's Research Portal

DOI:
10.1111/bph.14104

Document Version
Peer reviewed version

Link to publication record in King's Research Portal

Citation for published version (APA):
Fernandez-Chas, M., Curtis, M. J., & Niederer, S. A. (2018). Mechanism of doxorubicin cardiotoxicity evaluated by integrating multiple molecular effects into a biophysical model. *British Journal of Pharmacology*, *175*(5), 763-781. https://doi.org/10.1111/bph.14104

Citing this paper
Please note that where the full-text provided on King's Research Portal is the Author Accepted Manuscript or Post-Print version this may differ from the final Published version. If citing, it is advised that you check and use the publisher's definitive version for pagination, volume/issue, and date of publication details. And where the final published version is provided on the Research Portal, if citing you are again advised to check the publisher's website for any subsequent corrections.

General rights
Copyright and moral rights for the publications made accessible in the Research Portal are retained by the authors and/or other copyright owners and it is a condition of accessing publications that users recognize and abide by the legal requirements associated with these rights.

•Users may download and print one copy of any publication from the Research Portal for the purpose of private study or research.
•You may not further distribute the material or use it for any profit-making activity or commercial gain
•You may freely distribute the URL identifying the publication in the Research Portal

Take down policy
If you believe that this document breaches copyright please contact librarypure@kcl.ac.uk providing details, and we will remove access to the work immediately and investigate your claim.

Download date: 05. May. 2023

Mechanism of doxorubicin cardiotoxicity evaluated by integrating multiple molecular effects into a biophysical model

Running Title: Modelling Doxorubicin Cardiotoxicity in Silico

M Fernandez-Chas, M J Curtis, S A Niederer

Division of Imaging Sciences and Biomedical Engineering (MF, SAN) and Cardiovascular Division (MJC), King's College London, London SE1 7EH, UK

Address for Correspondence:

Dr Steven A. Niederer

Division of Imaging Sciences & Biomedical Engineering

The Rayne Institute

4th Floor, Lambeth Wing

St. Thomas' Hospital

Westminster Bridge Road

London SE1 7EH

Phone: 020 718 88299

Email: steven.niederer@kcl.ac.uk

ABSTRACT

Background and Purpose: Doxorubicin (DOX) is an effective cancer therapeutic agent but causes therapy-limiting cardiotoxicity. The effects of DOX and its metabolite doxorubicinol (DOXL) on individual channels have been well characterised in isolation. However, it is unknown how the action and interaction of affected channels combine to generate the phenotypic cardiotoxic outcome. We sought to develop an in silico model that links drug effects on channels to action potential duration (APD) and intracellular Ca^{2+} concentration in order to address this gap in knowledge.

Experimental Approach: We first propose two methods to obtain, from values reported in the literature, consensus drug effects on the currents of individual channels, transporters and pumps. Separately, we obtained equivalent values for APD and Ca^{2+} concentration (the readouts used as surrogates for cardiotoxicity). Once derived, the consensus effects on the currents were incorporated into established biophysical models of the cardiac myocyte and were refined adjusting the sarcoplasmic reticulum Ca^{2+} leak current (I_{Leak}) until the consensus effects on APD and Ca^{2+}

dynamics were replicated. Using factorial analysis, we then quantified the relative contribution of each channel to DOX and DOXL cardiotoxicity.

Key Results: The factorial analysis identified the rapid delayed rectifying K^+ current (I_{Kr}), the L-type Ca^{2+} current (I_{CaL}) and the sarcoplasmic reticulum Ca^{2+} leak current (I_{Leak}) as the targets primarily responsible for the cardiotoxic effects on APD and Ca^{2+} dynamics.

Conclusions and Implications: This study provides insight into the mechanisms of DOX induced cardiotoxicity and a framework for the development of future diagnostic and therapeutic strategies.

Abbreviations

AP, action potential; APD, action potential duration; DOX, doxorubicin; DOXL, doxorubicinol; I_{Kr}, rapid delayed rectifying K^+ current; I_{CaL}, L-type Ca^{2+} current; I_{Leak}, sarcoplasmic reticulum Ca^{2+} leak current; I_{NaK}, Na^+/K^+ pump current; I_{NaCa}, Na^+/Ca^{2+} exchange current; I_{Rel}, ryanodine receptor current; I_{Up}, sarcoplasmic reticulum Ca^{2+}-ATPase pump current; SR, sarcoplasmic reticulum.

INTRODUCTION

Anthracyclines play an important role in the treatment of neoplastic cancers due to their efficiency and broad activity spectrum. Doxorubicin (DOX) is the predominant anthracycline, but its use is limited due to cardiotoxicity (Octavia et al., 2012).

In humans, DOX cardiotoxicity manifests over two time scales: acute and chronic. Acute effects occur within 48 hours of infusion and are generally reversible and clinically manageable (Takemura & Fujiwara, 2007). They develop in up to 40% of the patient population and manifest as primary electrophysiological dysfunction: atypical ST-segment and T-wave abnormalities, reduced QRS voltages, sinus tachycardia, QT interval prolongation and ventricular and atrial arrhythmias (Octavia et al., 2012; Singal et al., 1987; Yeh et al., 2004). Chronic toxicity manifests as progressive hypotension, tachycardia with a characteristic decrease in the QRS voltage, cardiac dilatation and ventricular failure (Lefrak et al., 1973; Singal et al., 1987) and may not become evident until 4 to 20 years after the last administration of DOX (Octavia et al., 2012). Chronic toxicity affects >60% of patients receiving maximal acceptable cumulative dosages (Dresdale et al., 1983) and has a poor prognosis (Octavia et al., 2012; Takemura & Fujiwara, 2007). This combination of electrical and mechanical dysfunction represents cellular electrophysiology and excitation-contraction coupling toxicity.

Investigations on DOX toxicity mechanisms, whether after acute or chronic exposure, have made use of ex vivo isolated cardiac myocyte preparations. These studies have shown that changes in

action potential (AP) (Wang et al., 2001; Wang & Korth, 1995) and Ca^{2+} handling dynamics (Sag et al., 2011; Wang et al., 2001; Wang & Korth, 1995) in acute studies differ from outcomes after chronic exposure (Jensen, 1986; Shenasa et al., 1990). Based on this and the range of known effects on different relevant molecular targets, it can be surmised that acute and chronic DOX cardiotoxicity reflect a combination of direct DOX effects on channel, pump and exchanger function and indirect effects on expression levels, with the metabolite doxorubicinol (DOXL) which accumulates in cardiac tissue (Del Tacca et al., 1985) possibly contributing to the chronic toxicity (Olson & Mushlin, 1990). Unfortunately, although such a cause and effect matrix may be inferred, the mechanistic detail remains unclear.

Quantifying drug effects on relevant molecular targets may help inform earlier diagnosis of toxicity and better targeted treatment. Previous studies have primarily focused on characterising drug effects on individual molecular targets. How such effects account for the changes in AP and Ca^{2+} homeostasis is a gap in knowledge. Biophysical models of cellular electrophysiology and Ca^{2+} dynamics (Fink et al., 2011) may provide a framework for bridging this gap.

We have focused on modelling DOX and DOXL effects on electrophysiology and calcium handling. This is because these are important end effectors mediating adverse DOX and DOXL actions on rhythm and force. Changes in these effectors may be caused by direct drug-molecule interactions or may be secondary to known effects on mitochondrial DNA (Serrano et al., 1999), ROS production (Davies & Doroshow, 1986), the electron transport chain (Marcillat et al., 1989) and mitochondrial permeability (Montaigne et al., 2011). Whether the effects on ion channels and calcium handling are 'direct' or 'indirect' does not affect the modelling results, which incorporates 'end' effects and concentrations without the need to specify whether or not the outcomes are directly or indirectly mediated.

In this study, we modified two pre-existent mathematical models to investigate the contributions of different transporters, pumps and channels, hereafter called 'channels' when described collectively, to overall DOX and DOXL cardiotoxicity. The first task was to ensure standardization of the input data. Owing to the heterogeneity of the way drug effects are described in the literature, we undertook a parallel investigation to determine the best method to obtain a consensus drug effect on individual channels, APD and Ca^{2+} dynamics. The method of deriving and processing these effects is thus part of the study. Once derived, the consensus effect values for drug actions on channels were incorporated into biophysical models of cardiac myocyte electrophysiology and Ca^{2+} dynamics. We then refined the models until the consensus drug effect on APD and Ca^{2+} dynamics were replicated. Using factorial analysis, we then alternated the inclusion of individual consensus drug effects and their combinations to reveal the relative contribution of each channel, and their interactions, in mediating DOX and DOXL cardiotoxicity.

The study shows that biophysical modelling can replicate DOX cardiotoxicity well in both human and rabbit models, with some caveats. Using the models we make three testable predictions. First, that acute DOX and DOXL and chronic DOX exposure will increase the sarcoplasmic reticulum (SR) Ca^{2+} leak (I_{Leak}). Second, that reported increased K^+ permeability in cells chronically exposed to DOX is consistent with an increase in rapid delayed rectifying K^+ current (I_{Kr}). Third, that acute DOXL exposure is unlikely to cause inhibition of the Na^+/Ca^{2+} exchanger (I_{NaCa}).

METHODS

Cell Models

The bulk of the input data were from rabbit, and because of this, simulations were made for rabbit (Morotti et al., 2012) as well as human (ten Tusscher & Panfilov, 2006) models of cardiac ventricular myocyte electrophysiology and intracellular Ca^{2+} regulation. The independent variables in these models were the I_{Kr}, the L-type Ca^{2+} current (I_{CaL}), I_{Leak} and currents associated with the Na^+/K^+ pump (I_{NaK}), SR Ca^{2+}-ATPase (I_{Up}), I_{NaCa} (capable of operating in forward and reverse mode) and the ryanodine receptor (I_{Rel}). A full description of the model equations and parameters for both these models are available through the CellML repository (https://models.physiomeproject.org/workspace/49c) and were converted to C and MATLAB code through COR (http://opencor.ws/cor/) (Garny et al., 2003), now superseded by OpenCOR (http://opencor.ws).

In these models, the general form of the current through a given channel is as follows:

$$I_i = G_i(V - V_i) \qquad (1)$$

where I_i is the current through the channel, G_i is the channel conductance, V is the membrane potential and V_i is the Nernst potential for the channel.

The models simulate changes in currents during a simulated electrical field stimulation to generate values for AP and intracellular Ca^{2+} concentration. AP duration (APD) was expressed as ms at 90% repolarization and intracellular Ca^{2+} concentration was expressed as an absolute value at the systolic peak. We also determined the time in ms taken for the Ca^{2+} concentration to recover to 10% of its peak value (Ca^{2+} relaxation time), a variable that has been used in published literature as an index of recovery of diastolic Ca^{2+} concentration (Wang et al., 2001).

Drug Effects

The models allow variation in the influence of each current on AP and intracellular Ca^{2+} concentration, by using an α factor as follows:

$$I_i = \alpha_i G_i(V - V_i) \qquad (2)$$

where α_i is the consensus value for the effect of DOX (or DOXL) on each current.

Drug-induced changes in APD, systolic Ca^{2+} concentration and Ca^{2+} relaxation time were expressed as a % change from control values generated with $\alpha = 1$.

The consensus values of α, % change of APD, % change of systolic Ca^{2+} concentration and % change of Ca^{2+} relaxation time were determined by searching PubMed using the following keywords: doxorubucin, adriamycin, doxorubicinol, calcium, action potential, myocyte, ion currents, channels, pump, exchanger. Data selected for acute exposure of DOX and DOXL modeling were limited to cells exposed to the drug in vitro for up to 180 minutes. Data selected for simulating the chronic DOX exposure were limited to cells from hearts removed from subjects exposed chronically in vivo to DOX for a minimum of 1 week and a maximum of 9 weeks. These measurements reflect the combined effects of DOX and DOXL, which will both be present in the biophase, and their combined effects on protein targets are used to constrain the model. In studies where surrogate readouts of channel function were reported, these were treated as equivalent to direct measures. In the specific case where changes in channel mRNA expression were the primary information source, the fold change in mRNA between drug exposure and control was used as an estimate of the drug effect on function. The volume of available human tissue data was found to be insufficient for our purposes. Therefore, all data used to determine consensus effects were derived from dog, rabbit, guinea pig and rat. To avoid bias, no exclusion criteria based on data completeness, provenance or quality, were used with a single exception: rat data on APD was not included since rat ventricular APD is distinctively unrelated to I_{Kr} (Rees & Curtis, 1996).

We discovered that experimental methods and data reporting are very heterogeneous. Consequently, we evaluated two different methods for estimating the consensus effects of DOX and DOXL, i.e., values of α, % change of APD, % change of systolic Ca^{2+} concentration and % change of Ca^{2+} relaxation time.

Method 1

The first approach was based on an assumption that the maximum concentration used in a given study is the concentration causing the maximum effect on each given target. The values thus obtained therefore have accuracy but uncertain precision.

A single % change α value was calculated for each channel as the mean of the % change values reported from different studies rounded to the nearest 10%, ranging between 0.1 and 0.9 to represent a % change between 10% and 90% (Table 1, column 2). We used a similar approach when calculating the consensus values for the % change in APD, systolic Ca^{2+} concentration and Ca^{2+} relaxation time (Table 2, column 2).

This approach allows for the fact that a given drug concentration may have different effects in different preparations. However, this method disregards the concentration dependence of drug effects.

Unlike the α value for all other targets, the α value for I_{Leak} was fitted to achieve the consensus cellular Ca^{2+} transient and was not inferred from direct experimental measurements of I_{Leak}. This parameter is a prediction of the modelling framework and not an experimental measurement. The α for I_{Leak} is calculated as the factor needed for the simulated % systolic Ca^{2+} concentration to match the consensus % systolic Ca^{2+} concentration, with α bounded to fall between 2 and 10, representing a % increase ranging between 100% and 900%. Some qualitative data are available (Sag et al., 2011; Wang & Korth, 1995) that indicates a likely effect of DOX on this current, but no reliable quantitative values are available to date.

Method 2

The second approach was based on a different assumption: that drug inhibition or activation of each channel can be described by a Hill equation with no co-operativity, with the maximum effect of the drug (Emax) equalling 100% inhibition or a 100% increase. The values obtained have precision, but uncertain accuracy. The resulting scalars are given as:

$$\text{channel activity} = \frac{1}{1+\left(\frac{[\text{drug}]}{IC50}\right)^{\text{Hill}}}, \quad \text{channel activity} = \frac{1}{1+\left(\frac{EC_{50}}{[\text{drug}]}\right)^{\text{Hill}}} \qquad (3)$$

where IC_{50} or EC_{50} corresponds to the drug concentration that causes 50% inhibition or activation, respectively, [drug] is the concentration of the drug and Hill is the co-operativity parameter which is set to 1.

This approach allows EC_{50} or IC_{50} values to be estimated for all channels (Table 1, column 4-5; Table 2, column 3-4), even in cases where only a single data point was available. From this we were able to construct Hill plots that permitted estimation of % change in α after exposure to 100 μM of DOX and 10 μM of DOXL by extrapolation (Table 1, column 3). These concentrations were selected because they are direct counterparts of the concentrations most commonly evaluated in 'wet' tissue studies (Table 1 and Table 2, column 6). This method was not applied to estimate consensus values of % change of APD, systolic Ca^{2+} concentration and Ca^{2+} relaxation time as the concentrations in these studies are predominantly consistent with the chosen concentrations of 100 μM of DOX and 10 μM of DOXL.

The α values for I_{Leak} were estimated for the case of 100 μM of DOX and 10 μM of DOXL by first simulating the effect of DOX or DOXL to permit determination of an α value for I_{Leak}, which was inferred by fitting the model predictions of Ca^{2+} concentration to experimental measurements of Ca^{2+} concentration when cells were exposed to either 100 μM of DOX and 10 μM of DOXL. This gave α values for I_{Leak} for 100 μM of DOX and 10 μM of DOXL.

Chronic DOX exposure was not evaluated by this approach since changes in current activity develop over time and are not dose dependent in the classical sense owing to their genomic basis, and therefore not appropriately represented by a simple mass action model.

Provenance of Input Data and Methods for Best Estimation

The processes described above for determining consensus values were difficult to execute in certain cases. These cases included data that lacked precision (too few studies and/or semi quantitative estimates), or accuracy (several studies reporting contradictory estimates) as described below.

Estimates of % change of systolic Ca^{2+} concentration after acute DOX exposure

The change in systolic Ca^{2+} concentration caused by acute DOX exposure varies, with some authors reporting a decrease whilst others report an increase, e.g., Sag et al. (2011) reported a decrease of 43% whereas Wang & Korth (1995) reported a 50% increase. This inconsistency in response is also reflected in inotropy measurements which are equally inconsistent (De Beer et al., 2001). The +50% value was chosen as the consensus effect because the drug concentration used in this study (100μM) was the same as the reference concentration used in the acute DOX simulation.

Estimates of % change of Na^+/Ca^{2+} exchanger *inhibition after acute DOXL exposure*

Acute DOXL has been reported to cause up to 100% inhibition of the Na^+/Ca^{2+} exchanger (Table 1, column 2) (Boucek et al., 1987a) but when this effect was incorporated into the human and rabbit models the outcome was asystole due to failure of repolarisation. It is difficult to explore this observation further since the study (Boucek et al., 1987a) did not state whether the measurements were corrected for changes in intracellular Na^+ due to Na^+/K^+ pump inhibition.

In view of the potential importance of this, and the meagre provenance of the source data (Boucek et al., 1987a), we conducted a separate simulation to test if the reported 100% inhibition of the Na^+/Ca^{2+} exchanger could be explained by the secondary effect of intracellular Na^+ accumulation following the Na^+/K^+ pump inhibition by DOXL. To do this, we simulated the recovery of Ca^{2+} concentration following a caffeine exposure (a Na^+/Ca^{2+} exchanger-dependent process (Bers, 2000)) for the human cell model, with the Na^+/K^+ pump set at 50% (Table 1, column 2). This revealed that the published inhibition of the Na^+/Ca^{2+} exchanger can be explained by the inhibitory effects of accumulation of intracellular Na^+ due to Na^+/K^+ inhibition. For this reason, we deduced that DOXL has a negligible *direct* effect on the Na^+/Ca^{2+} exchanger and set α to 1 in the simulations that follow below.

Estimates of % change of APD after chronic DOX exposure

Chronic DOX experiments are fewer and the resultant α estimates are therefore less reliable than those for acute DOX exposure. Indeed, reported effects on APD are conspicuously inconsistent, with changes ranging from an increase of 10% (Milberg et al., 2007) to a decrease of ~20% (Doherty & Cobbe, 1990; Shenasa et al., 1990). We selected a -20% value as the consensus acute effect on APD.

Estimates of α value for I_{Kr} after chronic DOX exposure

Chronic DOX increases K^+ permeability (Shenasa et al., 1990) but the channel responsible has not been identified. We represented this qualitative observation by assuming, in the first instance, a 50% activation of the most commonly drug-affected repolarizing K^+ current, I_{Kr}. The limitations of this assumption are revisited in the Discussion.

Estimates of % change of systolic Ca^{2+} concentration after chronic DOX exposure

Data on effects of chronic DOX exposure on Ca^{2+} concentration suggest longer exposures cause an increase (Kapelko et al., 1996; Szenczi et al., 2005)(Kapelko et al., 1996; Szenczi et al., 2005) and shorter exposures cause a decrease (De Angelis et al., 2010). This may reflect chronic DOX causing a decrease in intracellular Ca^{2+} that gives rise to heart failure which then leads to Ca^{2+} accumulation (Olson & Mushlin, 1990) that is not seen with acute exposure.

As we are primarily interested in DOX toxicity, we aimed to simulate the decrease in Ca^{2+} concentration attributed to chronic DOX exposure (which has been examined only in rats to date). The idea of a decrease resonates with data from humans in which heart failure caused by chronic exposure to DOX has been associated with a depressed contractile state (Singal et al., 1987), which would be consistent with a reduction in Ca^{2+} concentration.

Simulations

The α values from method 1 were incorporated into human and rabbit models described above, and the resulting models labelled as acute DOX, chronic DOX and acute DOXL. Separately the α values from method 2 were incorporated and the models labelled as acute 100 μM DOX and acute 10 μM DOXL.

The field stimulation protocol used to generate APs consisted of 3,000 depolarizations at 1 Hz. This ensures equilibrium and is based on physiological and standard experimental pacing rate (Wang et al., 2001). APD, systolic Ca^{2+} concentration Ca^{2+} and relaxation time values for analysis were generated from the 3,001st depolarization.

We then compared the generated % change of APD, systolic Ca^{2+} concentration and relaxation time with the consensus values of the % change of APD, systolic Ca^{2+} concentration and Ca^{2+} relaxation time observed in experimental studies (Table 2, column 2). We then modified the consensus value of α for I_{Leak} (the explanation for this is given later) until we recapitulated the consensus % change values. A synopsis of predicted model function at different pacing rates for the final fitted models is provided in the online supplement.

Factorial Analysis

The overall process of computation ended with factorial analysis. APD, systolic Ca^{2+} concentration and Ca^{2+} relaxation time were generated by simulation with α values defined either as 1 (drug free simulation) or equal to the consensus values derived by method 1 and then by method 2 (consensus

altered simulation values). All combinations of α values (drug free and consensus altered value) were examined, thus revealing independent contributions of currents on APD, systolic Ca^{2+} concentration and Ca^{2+} relaxation. Current-current interactions were also considered by introducing simultaneous changes of α values in pairs of currents.

RESULTS

Acute DOX effects assessed by method 1

Rabbit

The APD, Ca^{2+} concentration and Ca^{2+} relaxation time were initially +4%, +174% and -1%, respectively, when there is no increase in the SR leak (α = 1 for I_{Leak}). Increasing the SR leak flux by +300% (α = 4 for I_{Leak}) caused the effect of simulated acute DOX on APD, Ca^{2+} concentration and Ca^{2+} relaxation time to be +7%, +23% and +17%, respectively, compared to consensus values of +50%, +50% and +30%, respectively (Figure 1, Table 2 and Table 3).

Human

The APD, Ca^{2+} concentration and Ca^{2+} relaxation time were initially +15%, +141% and +41%, respectively, when there is no increase in the SR leak (α = 1 for I_{Leak}). Increasing the SR leak flux by +100% (α = 2 for I_{Leak}) caused the effect of simulated acute DOX on APD, Ca^{2+} concentration and Ca^{2+} relaxation time to be +13%, +47% and +58%, respectively, compared to consensus values of +50%, +50% and +30%, respectively (Figure 1, Table 2 and Table 3).

Acute DOXL effects assessed by method 1

Rabbit

Estimates of APD, Ca^{2+} concentration and Ca^{2+} relaxation time were -28%, +11% and +44%, respectively. Since these values digress from the consensus values of -30%, -20% and +50%, respectively, leak flux was then increased by +900% (α = 10 for I_{Leak}). Consequently, APD, Ca^{2+} concentration and Ca^{2+} relaxation time became -24%, -29% and +57%, respectively, in closer agreement with the consensus values shown above (Figure 1, Table 2 and Table 3).

Human

Estimates of APD, Ca^{2+} concentration and Ca^{2+} relaxation time were -32%, -14% and +13%, respectively. Leak flux was then increased by +100% (α = 2 for I_{Leak}) and APD, Ca^{2+} concentration and Ca^{2+} relaxation time became -38%, -38% and +18%, respectively, in closer agreement with the consensus values of -30%, -20% and +50%, respectively (Figure 1, Table 2 and Table 3).

Chronic DOX effects assessed by method 1

Rabbit

Effects of chronic DOX on SR leak were set at +300% (α = 4 for I_{Leak}) in the rabbit model. The inclusion of these changes caused APD, Ca^{2+} concentration and Ca^{2+} relaxation time determined by method 1 to change from -14%, +87% and -13% to -11%, -12% and +9%, consistent with consensus values of -20%, -55% and +10%, respectively (Figure 1, Table 2 and Table 3).

Human

Effects of chronic DOX on SR leak were set at +200% (α = 3 for I_{Leak}) which caused APD, Ca^{2+} concentration and Ca^{2+} relaxation time determined by method 1 to change from -1%, +84% and +17% to -7%, -38% and +3%, consistent with consensus values of -20%, -55% and +10%, respectively (Figure 1, Table 2 and Table 3).

Acute DOX effects assessed by method 2

Rabbit

Method 2 predicted DOX-induced changes in APD, Ca^{2+} concentration and Ca^{2+} relaxation time, of +18%, +84% and -6% in rabbit, values that digress from the consensus values of +50%, +50% and +30%, respectively. When leak flux was increased by +100% (α = 2 for I_{Leak}) changes were +19%, +48% and +0%, respectively, in closer agreement with consensus values (Figure 1, Table 2 and Table 3).

Human

Method 2 predicted DOX-induced changes in APD, Ca^{2+} concentration and Ca^{2+} relaxation time, of +12%, +90% and +10%. When leak flux was increased by +100% (α = 2 for I_{Leak}), changes were +11%, +13% and +20%, respectively, in good agreement with consensus values +50%, +50% and +30%, respectively (Figure 1, Table 2 and Table 3).

Acute DOXL effects assessed by method 2

Rabbit

Method 2 predicted DOXL-induced changes in APD, Ca^{2+} concentration and Ca^{2+} relaxation time of -27%, +23%, +37% (rabbit) respectively. After leak was increased by +900% (α = 10 for I_{Leak}) values changed to -24%, -28% and +47%, respectively, in better agreement with consensus values of -30%, -20% and +50%, respectively (Figure 1, Table 2 and Table 3).

Human

Method 2 predicted DOXL-induced changes in APD, Ca^{2+} concentration and Ca^{2+} relaxation time of -30%, +6%, +7%, respectively. After leak was increased by +100% (α = 2 for I_{Leak}), values changed to -37%, -26%, and +13%, respectively, in closer agreement with consensus values of -30%, -20% and +50%, respectively (Figure 1, Table 2 and Table 3).

Factorial Analysis

We undertook factorial analysis on data for the human model only (Figure 3 and Table 4) having found that the simulation of drug effects in rabbit and human models were comparable (Figure 4).

Factorial analysis effects are expressed as % values (referring to the size of the change attributable to the current, or current interactions). We first considered the acute effects of DOX using method 1. In this case, the current with the greatest role in the effect of DOX on APD (method 1) was I_{CaL} (+7%) followed by I_{Kr} (+5%), with I_{Up}, I_{CaL}, I_{NaCa} and I_{Leak} having the largest role in the effect on Ca^{2+} concentration (-81%, +70%, -67% and -88%, respectively). I_{Up} had the largest role in the effect on Ca^{2+} relaxation time (+31%). Interactions with maximum role in the effect were ~~$I_{CaL}xI_{Nak}$ (1%), $I_{NaCa}xI_{Leak}$ (1%) and $I_{Nak}xI_{Leak}$ (1%) for APD,~~ $I_{Up}xI_{Leak}$ (23%) and $I_{Up}xI_{NaCa}$ (21%) for Ca^{2+} concentration and $I_{Up}xI_{NaCa}$ (7%) and $I_{NaCa}xI_{Leak}$ (6%) for Ca^{2+} relaxation time. All interactions for APD were negligible (<1%).

Method 2 outcomes were similar to method 1 outcomes. The current with the greatest role in the effect of DOX on APD using method 2 was I_{CaL} (+5%) followed by I_{Kr} (+6%), with I_{CaL} and I_{Leak} having the most substantial role in the effects on Ca^{2+} concentration (+50% and -72%, respectively). In contrast, Ca^{2+} relaxation time was affected by I_{Leak} only (+15%). Interactions with maximum roles in the effect were ~~$I_{CaL}xI_{Leak}$ (1%) and $I_{Rel}xI_{Leak}$ (1%) for APD,~~ $I_{CaL}xI_{Leak}$ (13%) for Ca^{2+} concentration and $I_{Rel}xI_{Leak}$ (3%) for Ca^{2+} relaxation time. All interactions for APD were negligible (<1%).

Next, we considered acute effects on DOXL. In method 1, changes in APD were predominantly determined by effects on I_{NaK}, I_{Up}, I_{Kr} and I_{Leak} (-15%, -9%, -7% and -6%, respectively), with effects on I_{NaK}, I_{Up} and I_{Leak} contributing the most to changes in Ca^{2+} concentration (+145%, -113% and -79%, respectively) and changes in Ca^{2+} relaxation time (-13%, +24% and +9%, respectively). Interactions with maximum influence were effects on $I_{Up}xI_{NaK}$ (7%) for changes in APD, effects on $I_{Up}xI_{NaK}$ (85%) for changes in Ca^{2+} concentration and effects on $I_{Up}xI_{Leak}$ (8%) for changes in Ca^{2+} relaxation time.

In method 2, acute effects of DOXL exposure were accounted for by actions on targets that are in close agreement with findings for method 1, with effects on I_{NaK}, I_{Up}, I_{Kr} and I_{Leak} (-14%, -8%, -7% and -7%, respectively), I_{NaK}, I_{Up} and I_{Leak} (+161%, -118% and -87%, respectively) and I_{NaK}, I_{Up} and I_{Leak} (-13%, +18% and +9%, respectively) having the major role in the effects on APD, Ca^{2+} concentration and Ca^{2+} relaxation time, respectively. Interactions with maximum influence were $I_{Up}xI_{NaK}$ (7%) for APD, $I_{Up}xI_{NaK}$ (82%) for Ca^{2+} concentration and $I_{Up}xI_{NaK}$ (5%) for Ca^{2+} relaxation time.

Finally, we considered effects of chronic DOX exposure. Here, effects on I_{Kr} (-6%), I_{CaL} (+5%) and I_{Leak} (-4%), played the predominant role in changes in APD (similar to findings for effects of acute DOX exposure). Effects on I_{CaL} and I_{Leak} had the major contribution to changes in Ca^{2+}

concentration (+46% and -109%, respectively) whilst effects on I_{NaCa} and I_{Leak} had the greatest contribution to changes in Ca^{2+} relaxation time (+9% and +13%, respectively). Interactions having the greatest contribution to effects were ~~$I_{Nak}xI_{Leak}$ (1%) for APD,~~ $I_{CaL}xI_{Leak}$ (23%) for Ca^{2+} concentration and $I_{Rel}xI_{Leak}$ (10%) for Ca^{2+} relaxation time. All interactions for APD were negligible (<1%).

Testing Model Assumptions

While the effects of DOX on the heart have been studied extensively, we have shown that these measurements are very heterogeneous spanning a broad range of species, preparations and temperatures. We have proposed and applied two frameworks for quantitatively combining heterogeneous pharmacological data. However a number of assumptions, indirect inferences and simplifications were required to combine all of the experimental data. Here we have performed additional simulations to interrogate whether these assumptions are robust.

Acute DOX causes a decrease in heart rate (Suzuki et al., 1997). To explore whether bradycardia affects the modelling we imposed a large reduction in rate (to 0.5 Hz) and found a range of modifications in outcome. There was no particular pattern within or between human and rabbit comparisons. However, given that the derived default model used 1Hz stimulation (for reasons explained) and yet 1 Hz is severely bradycardic for rabbit while normal for human, and given that baseline Ca^{2+} and Na^{+} values are highly heart rate dependent, and this dependence is species related, it is no surprise that the effects of this severe bradycardia differed from setting (e.g. acute DOX, human) to setting (e.g., chronic DOX, rabbit) (Table 5).

In the online supplement we present the frequency dependence of drug effects in the human and rabbit models. Frequency did not qualitatively effect the model results (e.g. for acute DOX APD, peak Ca^{+} and Ca^{2+} RT all increased). However, for a number of models there was a marked impact on diastolic Ca^{2+} and intracellular Na^{+} frequency response. In the majority of cases there is no reverse rate dependence, the exception being the DOX 100μM rabbit model. There are insufficient wet biology data sets to examine these model predictions, and whether they reflect outcomes in human or rabbits will require experimental validation.

The level of I_{NaCa} inhibition in the simulations of acute exposure to DOX was derived from a combination of the available experimental measurements from the three relevant publications. Two values were from rabbit and one was from canine studies (Table 1). Considering the mean of only the rabbit measurements would give an inhibition of I_{NaCa} of 10% instead of the original 40% consensus value derived from the mean of the three studies. The simulation outcomes for rabbit are not strongly affected by the level of I_{NaCa} inhibition (Table 5). However, in the human model, while the effect of DOX on APD remained unchanged, the level of I_{NaCa} inhibition by DOX did affect the

Ca^{2+} transient (Table 5). This may be due to the greater increase in SR leak flux in the rabbit model resulting in an already attenuated Ca^{2+} transient that is less dependent on I_{NaCa}.

Estimations for DOX inhibition of I_{Kr} were based in part from guinea pig measurements performed by Wang and Korth (1995) who found that DOX caused a 40% inhibition of what they called 'IK'. Because I_{Ks} is up to ten times larger than I_{Kr} in guinea pigs (Sanguinetti & Jurkiewicz, 1990) it cannot be assumed that the Wang and Korth effects are entirely attributable to I_{Kr} block (these investigators used tail current as their readout and the work was done before it was mandatory to disentangle I_{Kr} from I_{Ks}) meaning that relying on their data alone may overestimate the effect of DOX on I_{Kr}. Fortunately, in an expression system Ducroq et al. (2010) reported that DOX had an IC50 for I_{Ks} of ~5μM and limited inhibition of I_{Kr} at a DOX concentration of 30μM. With these two (albeit limited) estimates of effects, we tested the impact of potentially over estimating DOX effects on I_{Kr} by running simulations with the α value of I_{Kr} set to -30%, -20% and -10%. The results are presented in Table 5. In all simulations decreasing the inhibition of I_{Kr} decreased the prolongation of the APD, making the model less able to recapitulate the experimentally measured effects of DOX on APD. To test if blocking I_{Ks} as opposed to or in combination with I_{Kr} alters the predicted effect of DOX, we simulated the impact of I_{Kr} and I_{Ks} inhibition in the DOX 100μM model in two simulations. First we assumed that I_{Kr} was not inhibited by DOX and that I_{Ks} inhibition has an IC50 of 5μM. In the second simulation we assumed I_{Kr} had an IC50 of 100μM (significantly larger than 30μM and causing a -50% inhibition of I_{Kr} inferred from Wang and Korth (1995)) and I_{Ks} had an IC50 of 5μM. The predicted effects on cellular function are reported in Table 5 and show that all combinations of possible K^+ channel inhibition due to acute DOX exposure predict changes in APD and the Ca^{2+} transient consistent with consensus values.

The input data for I_{Kr} effects in the simulations of chronic DOX relied on potassium permeability data (Shenasa et al., 1990) as a surrogate since no direct data on I_{Kr} exists. We made the assumption that chronic DOX caused an increase of I_{Kr} of +50%. To test the impact of this assumption we performed simulations with the α value for I_{Kr} varying from 0% and +25% and reported the results in Table 5. Although this decreased the ability of the simulations to predict DOX effects on APD and Ca^{2+} concentration the changes were small, indicating that the uncertainty in this parameter is unlikely to alter our study conclusions.

DISCUSSION

In this study we showed for the first time that it is possible for two well-known mathematical models of rabbit and human ventricular electrophysiology, when provided with appropriate scaling factors, to replicate the consensus effects of acute DOX, chronic DOX and acute DOXL exposure on APD, systolic Ca^{2+} concentration and Ca^{2+} relaxation time. The consensus values were

determined using a novel combination of two different methods. Reassuringly, they generated similar predictions of the drug effect on APD, Ca^{2+} concentration and Ca^{2+} relaxation time.

The process of model development identified the need to introduce drug effects on the SR Ca^{2+} leak to recapitulate observed drug induced changes in cellular function, including the increase in K^+ permeability following chronic DOX exposure that is consistent with DOX effects on I_{Kr}, and also showed that acute DOXL exposure is unlikely to inhibit $I_{NaCa.}$

Using the models we quantified the relative contributions of drug effects on each target to the toxic phenotype. Consideration of the scaling factors revealed that the consensus drug effects were different for simulation of acute DOX, compared with chronic DOX and acute DOXL exposure.

I_{NaCa} inhibition

The modelling indicates that reports that I_{NaCa} is inhibited by DOXL (Olson et al., 1988) by up to 100% may not be correct (or, at least, relevant to the clinical use of the drug, owing perhaps to the selection of inappropriately high drug concentrations for study, an issue revisited at the end of the discussion). Unfortunately, it is not possible to interrogate this in detail since Boucek et al (1987a). did not reveal whether the effects of elevated intracellular Na^+ that result from DOXL inhibiting the Na^+/K^+ pump were accounted for. Our simulation of Ca^{2+} concentration following a caffeine exposure and inhibition of the Na^+/K^+ pump (Figure 2) suggests the increase in Na^+ would inhibit the activity of the Na^+/Ca^{2+} exchanger and therefore we cannot assume that, in a functioning cell, the effects of DOXL on the Na^+/Ca^{2+} exchanger current would result exclusively from direct effects.

SR Leak

The introduction in the modelling of an increase in SR leak due to DOX and DOXL allowed the models to replicate consensus APD and Ca^{2+} 'wet' values. The estimated increase in SR leak was approximated from qualitative observations (Sag et al., 2011; Wang & Korth, 1995) and is potentially due to an increase in reactive oxygen species production that is known to increase SR leak (Bers, 2014) an effect caused by DOX (Octavia et al., 2012; Terentyev et al., 2008) .

The SR leak was fitted to achieve the experimentally observed change in systolic Ca^{2+} concentration. In the acute DOX studies, systolic Ca^{2+} was reported to increase and decrease in two different publications. We choose the 50% increase in Ca^{2+} as the consensus value as it was recorded at the reference DOX concentration (100μM). Had we aimed to fit the SR leak to achieve a 40% decrease in systolic Ca^{2+} the magnitude of SR leak would have needed to be increased even further, indicating that the current estimates of increase SR leak flux may be conservative.

The wide range of SR leak predicted by the model may reflect true differences in leak for different drugs under different conditions. The magnitudes, 2-10 fold, are within the range of reported changes in SR leak or surrogate measures in response to pharmacological agents, disease and in genetic models. (~2-6 fold) (Kohlhaas et al., 2006; Terentyev et al., 2008). At the same time the SR leak was inferred to maximise the similarity between the model predictions and experimentally observed cellular readouts. This means that all uncertainty and error in the drug effects on all the channels will be accumulated in this fitted parameter. This has the potential to increase the variability in the absolute magnitude of the change in the leak, however, the consistent qualitative finding of increased leak flux supports this model prediction.

APD

DOX and DOXL are known to affect multiple channels after exposure to acute DOX

(Boucek et al., 1987a; Boucek et al., 1987b; Caroni et al., 1981; Earm et al., 1994; Miwa et al., 1986; Mushlin et al., 1993; Olson et al., 1988; Qing et al., 1991; Sag et al., 2011; Wang & Korth, 1995), chronic DOX (Arai et al., 1998; Dodd et al., 1993; Huang et al., 2003; Keung et al., 1991; Olson et al., 2005; Shenasa et al., 1990)and acute DOXL (Boucek et al., 1987a; Boucek et al., 1987b; Mushlin et al., 1993; Wang et al., 2001). However, we found that not all effects are important for determining the cardiotoxicity.

The factorial analysis revealed that actions on I_{Up}, $I_{NaK,}$ I_{Kr} and I_{Leak} were responsible for the majority of acute DOXL effects on APD, whereas actions on I_{Up}, I_{NaK} and I_{Leak} resulted in the changes in systolic Ca^{2+} concentration. In contrast, actions on I_{CaL} and I_{Kr} were identified as the principal determinants of the effects of acute and chronic DOX on APD, with I_{Leak} also affecting the APD in chronic DOX. Actions on I_{CaL} and I_{Leak} were identified as the principal determinants of their effects on systolic Ca^{2+} concentration in acute and chronic DOX, with I_{Up} and I_{NaCa} also having an effect in acute DOX. This analysis therefore identifies I_{Kr}, I_{CaL} and I_{Leak} as the channels to be targeted for preventive intervention or early detection of DOX cardiotoxicity, with I_{Up} and I_{NaK} also relevant owing to the effects of DOXL.

The importance of effects on multiple ion currents, specifically I_{Kr} and $I_{CaL,}$ in determining changes in APD is consistent with findings from previous modelling (Mirams et al., 2011) and single cell experimental studies(Kramer et al., 2013).

We showed that DOX- and DOXL-induced increases in α for I_{Leak} were necessary for optimal predictiveness, regardless of the model. In all cases the increased leak depleted the SR of Ca^{2+} and lowered the systolic Ca^{2+} concentration. Additionally, and importantly, it also caused a shortening of the APD (Table 4). This may explain the counterintuitive finding that these I_{Kr} blocking drugs shorten APD (see above). I_{Leak} does not act directly on the transmembrane potential but due to the

decrease in SR load and the subsequent decrease in systolic Ca^{2+} concentration there will be a decrease in I_{NaCa} flux that in turn shortens the APD (Janvier & Boyett, 1996).

I_{NaK} was found to play a role in the APD effects of acute exposure to DOXL. Inhibition of I_{NaK} causes an increase in intracellular Na^+ concentration reducing the electrochemical gradient driving Ca^{2+} entry via $I_{NaCa.}$ accounting for the positive inotropic effect of I_{NaK} blockade (Altamirano et al., 2006) and the known effects of acute DOXL (Bueno-Orovio et al., 2014) on Ca^{2+} and APD (Table 4).

The large changes in α for I_{Rel} (Table 1, column 2) did not account for the acute or chronic DOX effects on APD or systolic Ca^{2+} concentration. The inability of I_{Rel} to change the Ca^{2+} concentration is as predicted from other studies (Eisner et al., 2013) and can be explained by the fact that increasing or decreasing I_{Rel} will cause a subsequent decrease or increase in SR Ca^{2+} uptake which in turn functionally antagonises the effect of changes in I_{Rel} on Ca^{2+} concentration.

Role of effects of DOXL in mediating the effects of chronic DOX exposure

The metabolism of DOX under clinical conditions to produce DOXL means that the heart will be exposed to both compounds, albeit in concentrations that will vary in absolute terms and in terms of concentration ratios, both in the short term (over a day) and in the long term. We have not simulated the dynamic changing exposure of the heart to DOX and DOXL concentrations nor have we attempted to model a specific DOX to DOXL absolute or relative concentration. However, to create a representative simulation of chronic DOX exposure we combined multiple measurements (unavoidably derived from different species) exposed to 1 to 9 weeks of DOX. To examine which of the two compounds is likely to exert the dominant effect on any variable, we compared individual effects for in-vivo DOX exposure with the individual effects for in-vitro DOX and DOXL exposure (Fig. 3).

Our modelling study predicts that despite the similarity between chronic DOX and acute DOXL models in terms of changes in APD and systolic Ca^{2+} concentration (Figure 1), their effects on individual channels appear to be different (Figure 3). This means that DOXL accumulation is unlikely to explain the toxicity of chronic DOX exposure, consistent with the findings of Mushlin et al. (Mushlin et al., 1993). Likewise, the effect of acute DOX and chronic DOX on channels is similar yet they have different effects on APD and systolic Ca^{2+} concentration (Figure 3). This finding suggests studying the effects of acute DOX could be useful for predicting the toxic effect of the chronic exposure to DOX.

Clinical relevance

In order to interrogate the clinical relevance of the findings, it is useful to consider concentration-dependence. However, the pertinent concentration may not be the plasma concentration, owing to possible accumulation of drug inside cells and other factors.

The range of acute DOX IC_{50}/EC_{50} values for channel effects derived from cellular preparations from the literature were between 29 and 7251 μM (Table 1, column 4), while the IC50 values derived for DOX for I_{Ks} in an expression system were ~5 μM, and the equivalent derived values for effects on APD, systolic Ca^{2+} concentration and Ca^{2+} relaxation time were 92 to 233 μM (Table 2, column 3, with one published value (Sag et al., 2011) excluded as explained). Similarly, estimates of DOXL IC_{50} and EC_{50} values were 8 - 240 μM for channel effects and 30 - 92 μM for effects on APD, systolic Ca^{2+} concentration and Ca^{2+} relaxation time (Table 1, column 4 and Table 2, column 3, respectively).

The DOX peak plasma concentrations in the clinical setting are reported as 1 - 10 μM (Barpe et al., 2010; Cummings & Smyth, 1988; Gianni et al., 1997) and the equivalent value for DOXL is 0.2 μM (Cummings & Smyth, 1988). With the exception of reported I_{Ks} inhibition (Ducroq et al., 2010), these plasma levels are somewhat lower than those required to obtain channel effects and actions on APD, Ca^{2+} concentration and Ca^{2+} relaxation time, according to the experimental pharmacology literature. One explanation for this mismatch is that the acute cardiac toxicity associated with DOX in vivo may not be attributable to the acute ion channel effects. Alternatively, intracellular drug accumulation may be the primary determinant of the cardiotoxicity, as suggested previously (Olson et al., 1974), meaning that plasma concentration may not be indicative of the active concentration. A third explanation is the possible existence of an unknown DOX metabolite that accounts for the toxicity. Finally, the low IC50 value reported for I_{Ks} (compared with reported IC50 values for other targets) raises the possibility that I_{Ks} block is the primary contributor to acute DOX toxicity. In the online supplement we provide reference simulations of I_{Kr} inhibition alone or I_{Ks} inhibition alone in the human and rabbit models. For a 50% inhibition of I_{Ks}, (occurring at a clinically relevant drug concentration), the rabbit model shows negligible effects (all changes <3%). In contrast the human model shows a much larger response (changes range from 5-28%). It would appear from these findings that the role of I_{Ks} in mediating some of DOX's cardiotoxicity may have been underestimated, and our recommendation would be that this be given more consideration going forward.

We should note that plasma concentrations after a single dose do not give insight into the concentration-dependence of chronic toxicity.

In summary, the present findings illustrate that the majority of published data on DOX and DOXL IC_{50}/EC_{50} values for individual channels and none of the cellular function IC_{50}/EC_{50} values directly relate to macro cardiac toxicity in terms of concentration dependence. This is not likely to be

resolved until an exact matching data set of in vivo and channel actions is available, one in which exposure times are identical, and free drug concentrations and cell accumulation over time are better characterised. Nevertheless, the models provide a novel tool for linking channel effects to cellular phenotypes, despite the limitations inherent to the data. This study is therefore a first step towards linking channel effects to multi-scale emergent cellular phenotypes.

Limitations and Future directions

A novel combination of two proposed data integration methodologies was proposed to provide a rational framework for data integration. In the current version we treat each experimental read out as independent and ignore the variability of measurements. Specifically, we have not made any assumptions about whether two or more observations derive from a single protocol or separate protocols, and we do not place more weight on measurements that are less variable. This is exemplified by the acute effects of DOX on I_{CaL} where Wang and Korth (1995) report a mean 21% increase in I_{CaL}. However, when the mean changes were interpreted in the context of the variation in the experimental measurements, they were reported to not be statistically significant (Wang and Korth, 1995). Further, while reporting no significant change in I_{CaL} Wang and Korth, (1995) these investigators reported a significant increase in peak Ca^{2+} concertation and APD. Hence, while we include the values from this study, our approach does not necessarily generate conclusions that are consistent with Wang and Korth experimental results.

Data from across all species was used to inform the model. The majority of data is available from rabbit preparations, however, key measurements are not recorded in rabbit. Specifically, none of the cellular readouts were recorded in rabbit for acute DOX or DOXL and the effect of chronic DOX on I_{CaL} was not recorded in rabbit, despite being identified as an important contributor to chronic DOX effects on APD. This means there was not a complete species specific data set for any of the drug conditions we studied and so we have assumed species differences were small.

The effects of acute DOX on K^+ currents and the consequences in terms of APD alterations are contentious issues. The outcomes of modelling are reasonably consistent and predict that acute DOX will cause APD prolongation, regardless of whether inhibition of I_{Kr} or I_{Ks} is the predominant effect of DOX on K^+ currents. The findings from studies that measure K^+ currents are however somewhat inconsistent and contradictory. Thus, Wang and Koth (1995) reported that acute DOX causes inhibition of I_{Kr}, whereas Ducroq et al. (2010) reported that acute DOX inhibits I_{Ks} and not I_{Kr}. In neither study was it possible to infer whether APD effects were the result in whole or part from block of either current. When the effect of acute DOX toxicity on K^+ currents was modelled using the Ducroq et al IC50 values for I_{Kr} and I_{Ks} (or the IC50 value for I_{Ks} alone) there was a pronounced increase in APD, an effect more consistent with the consensus reported changes in APD compared with when no effect of DOX on I_{Ks} was included in the modeling. Unfortunately the

effect of I_{Ks} inhibition on APD in the absence of I_{Kr} inhibition is unclear, with no effect found in human (Jost et al., 2005) or rabbit (Lengyel et al., 2001) ventricular myocytes yet, in contrast, APD prolongation was found in human and rabbit ventricular myocytes by other investigators (Bosch et al., 1998)(Lu et al., 2001). Separately, the simulated effect of I_{Ks} inhibition varies from one human cardiac myocyte cell model to the next (Mirams et al., 2014) with the ten Tusscher model used in the present study exhibiting a far greater APD sensitivity to I_{Ks} inhibition than other models. These confounding factors mean that it is not possible to conclude if DOX predominantly effects I_{Ks} or I_{Kr} from simulation results alone. Nevertheless, and importantly, varying the specific effect of acute DOX on K^+ currents did not qualitatively alter our prediction that acute DOX increases SR leak. Regardless of the simulated effect of acute DOX on K^+ currents (inhibiting I_{Ks} only or inhibiting both I_{Ks} and I_{Kr}), for both human and rabbit models the simulated results were closer to experimental measurements if SR leak was increased (see online supplement).

We have made use of only two cardiac myocyte models (rabbit and human) for interpreting our results. Others have proposed using species-dependent methods for interpreting pre-clinical data in species specific models (O'Hara & Rudy, 2011). However, insufficient data were available for any of the compounds we studied to attempt this level of specificity.

We have assumed that the Hill coefficient is equal to 1 for all targets for both drugs. There are limited measurements of the Hill coefficient and cooperative inhibition is a possibility. However, Boucek et al., (1987b) did find that the slope of their Dixon plots were for doxorubicin inhibition of I_{NaK} and I_{Up}, consistent with a Hill coefficient of 1.

Finally, we have simulated cellular phenotypes as surrogates for measures of organ scale function. Simulating full heart electro-mechanics and pseudo ECGs may provide further insight into the link between changes in cellular function and clinical readouts.

Conclusions

We have presented the first model to capture the effects of DOX on cardiac electrophysiology and Ca^{2+} handling in the human and the rabbit incorporating acute and chronic effects as well as effects of the DOX metabolite DOXL. The human and rabbit models reproduce qualitative changes in APD and Ca^{2+} concentration morphology. For future reference, our simulations predict three important actions of DOX that require confirmation by pharmacological experimentation. These are (i) the apparent importance of an hitherto unhearalded increase in SR Ca^{2+} leak flux, (ii) the apparent unimportance of acute DOXL effects on I_{NaCa} and (iii) the inference that the increased K^+ permeability caused by chronic DOX exposure results from an increase in I_{Kr}.

The factorial analysis shows that a limited number of changes to specific channels may explain the majority of drug effects on cellular function and that changes in Ca^{2+} dynamics are caused by DOX and DOXL acting directly on Ca^{2+} handling and are not a secondary effect caused by changes in AP.

The current modelling approach provides a means of testing the relevance of single target effects in determining the cardiotoxic phenotype, and in the case of DOX, emerging information on timecourses of effects and drug accumulation in cells can be incorporated to provide refinement and greater insight.

Author Contributions

MF performed the experiments, SAN and MJC designed the study and experiments, and all three wrote the manuscript.

Acknowledgements

This study was supported by the Daphne Jackson Trust, the Royal Academy of Engineering and King's College London. The research leading to these results has received funding from the European Community's Seventh Framework Programme (FP7/2007-2013) under Grant Agreement Number 602156 - HeCaToS. The research was supported by the National Institute for Health Research Biomedical Research Centre, the Wellcome EPSRC Centre for Medical Engineering (WT 203148/Z/16/Z) and the British Heart Foundation award (RE/08/003) at King's College London.

Conflicts of Interest: None.

References

Altamirano J, Li Y, DeSantiago J, Piacentino V, Houser SR, & Bers DM (2006). The inotropic effect of cardioactive glycosides in ventricular myocytes requires Na+-Ca2+exchanger function. The Journal of Physiology 575: 845-854.

Arai M, Tomaru K, Takizawa T, Sekiguchi K, Yokoyama T, Suzuki T, et al. (1998). Sarcoplasmic reticulum genes are selectively down-regulated in cardiomyopathy produced by doxorubicin in rabbits. Journal of Molecular and Cellular Cardiology 30: 243-254.

Barpe DR, Rosa DD, & Froehlich PE (2010). Pharmacokinetic evaluation of doxorubicin plasma levels in normal and overweight patients with breast cancer and simulation of dose adjustment by different indexes of body mass. European Journal of Pharmaceutical Sciences 41: 458-463.

Bers DM (2000). Calcium fluxes involved in control of cardiac myocyte contraction. Circulation Research 87: 275-281.

Bers DM (2014). Cardiac Sarcoplasmic Reticulum Calcium Leak: Basis and Roles in Cardiac Dysfunction. Annual Review of Physiology 76: 107-127.

Boucek RJ, Kunkel EM, Graham TP, Brenner D, & Olson RD (1987a). Doxorubicinol, the metabolite of doxorubicin, is more cardiotoxic than doxorubicin. Pediatr Res 21: 187A-187A.

Boucek RJ, Olson RD, Brenner DE, Ogunbunmi EM, Inui M, & Fleischer S (1987b). The major metabolite of doxorubicin is a potent inhibitor of membrane-associated ion pumps. A

correlative study of cardiac muscle with isolated membrane fractions. Journal of Biological Chemistry 262: 15851-15856.

Bueno-Orovio A, Sánchez C, Pueyo E, & Rodriguez B (2014). Na/K pump regulation of cardiac repolarization: insights from a systems biology approach. Pflugers Arch - Eur J Physiol 466: 183-193.

Caroni P, Villani F, & Carafoli E (1981). The cardiotoxic antibiotic doxorubicin inhibits the Na + /Ca 2+ exchange of dog heart sarcolemmal vesicles. FEBS Letters 130: 184-186.

Cummings J, & Smyth JF (1988). Pharmacology of adriamycin: The message to the clinician. European Journal of Cancer and Clinical Oncology 24: 579-582.

Davies KJ, & Doroshow JH (1986). Redox cycling of anthracyclines by cardiac mitochondria. I. Anthracycline radical formation by NADH dehydrogenase. Journal of Biological Chemistry 261: 3060-3067.

De Angelis A, Piegari E, Cappetta D, Marino L, Filippelli A, Berrino L, et al. (2010). Anthracycline cardiomyopathy is mediated by depletion of the cardiac stem cell pool and is rescued by restoration of progenitor cell function. Circulation 121: 276-292.

De Beer EL, Bottone AE, & Voest EE (2001). Doxorubicin and mechanical performance of cardiac trabeculae after acute and chronic treatment: a review. European Journal of Pharmacology 415: 1-11.

Del Tacca M, Danesi R, Ducci M, Bernardini C, & Romanini A (1985). Might adriamycinol contribute to adriamycin-induced cardiotoxicity? Pharmacological Research Communications 17: 1073-1084.

Dodd DA, Atkinson JB, Olson RD, Buck S, Cusack BJ, Fleischer S, et al. (1993). Doxorubicin cardiomyopathy is associated with a decrease in calcium release channel of the sarcoplasmic reticulum in a chronic rabbit model. Journal of Clinical Investigation 91: 1697-1705.

Doherty JD, & Cobbe SM (1990). Electrophysiological changes in animal model of chronic cardiac failure. Cardiovascular Research 24: 309-316.

Dresdale A, Bonow RO, Wesley R, Palmeri ST, Barr L, Mathison D, et al. (1983). Prospective evaluation of doxorubicin-induced cardiomyopathy resulting from postsurgical adjuvant treatment of patients with soft tissue sarcomas. Cancer 52: 51-60.

Ducroq J, Moha ou Maati H, Guilbot S, Dilly S, Laemmel E, Pons-Himbert C, et al. (2010). Dexrazoxane protects the heart from acute doxorubicin-induced QT prolongation: a key role for I(Ks). British Journal of Pharmacology 159: 93-101.

Earm YE, Ho W-K, & So I (1994). Effects of Adriamycin on Ionic Currents in Single Cardiac Myocytes of the Rabbit. Journal of Molecular and Cellular Cardiology 26: 163-172.

Fink M, Niederer SA, Cherry EM, Fenton FH, Koivumäki JT, Seemann G, et al. (2011). Cardiac cell modelling: observations from the heart of the cardiac physiome project. Progress in biophysics and molecular biology 104: 2-21.

Gianni L, Viganò L, Locatelli A, Capri G, Giani A, Tarenzi E, et al. (1997). Human pharmacokinetic characterization and in vitro study of the interaction between doxorubicin and paclitaxel in patients with breast cancer. Journal of Clinical Oncology 15: 1906-1915.

Huang X-m, Zhu W-h, & Kang M-l (2003). Study on the effect of doxorubicin on expressions of genes encoding myocardial sarcoplasmic reticulum Ca2+ transport proteins and the effect of taurine on myocardial protection in rabbits. Journal of Zhejiang University 4: 114-120.

Janvier NC, & Boyett MR (1996). The role of Na-Ca exchange current in the cardiac action potential. Cardiovascular Research 32: 69-84.

Jensen RA (1986). Dororubicin cardiotoxicity: contractile changes after long-term treatment in rat. The Journal of Pharmacology and experimental therapeutics 236: 197-203.

Kapelko VI, Williams CP, Gutstein DE, & Morgan JP (1996). Abnormal Myocardial Calcium Handling in the Early Stage of Adriamycin Cardiomyopathy. Archives of Physiology and Biochemistry 104: 185-191.

Keung EC, Toll L, Ellis M, & Jensen RA (1991). L-type cardiac calcium channels in doxorubicin cardiomyopathy in rats morphological, biochemical, and functional correlations. Journal of Clinical Investigation 87: 2108-2113.

Kohlhaas M, Zhang T, Seidler T, Zibrova D, Dybkova N, Steen A, et al. (2006). Increased Sarcoplasmic Reticulum Calcium Leak but Unaltered Contractility by Acute CaMKII Overexpression in Isolated Rabbit Cardiac Myocytes. Circulation Research 98: 235-244.

Kramer J, Obejero-Paz CA, Myatt G, Kuryshev YA, Bruening-Wright A, Verducci JS, et al. (2013). MICE Models: Superior to the HERG Model in Predicting Torsade de Pointes. Scientific Reports 3.

Lefrak EA, Piťha J, Rosenheim S, & Gottlieb JA (1973). A clinicopathologic analysis of adriamycin cardiotoxicity. Cancer 32: 302-314.

Marcillat O, Zhang Y, & Davies KJA (1989). Oxidative and non-oxidative mechanisms in the inactivation of cardiac mitochondrial electron transport chain components by doxorubicin. Biochemical Journal 259: 181-189.

Milberg P, Fleischer D, Stypmann J, Osada N, Mönnig G, Engelen MA, et al. (2007). Reduced repolarisation reserve due to anthracycline therapy facilitates torsade de pointes induded by Ikr blockers. Basic Research in Cardiology 102: 42-51.

Mirams GR, Cui Y, Sher A, Fink M, Cooper J, Heath BM, et al. (2011). Simulation of multiple ion channel block provides improved early prediction of compounds' clinical torsadogenic risk. Cardiovascular Research 91: 53-61.

Miwa N, Kanaide H, Meno H, & Nakamura M (1986). Adriamycin and altered membrane functions in rat hearts. Br J Exp Pathol 67: 747-755.

Montaigne D, Marechal X, Preau S, Baccouch R, Modine T, Fayad G, et al. (2011). Doxorubicin induces mitochondrial permeability transition and contractile dysfunction in the human myocardium. Mitochondrion 11: 22-26.

Morotti S, Grandi E, Summa A, Ginsburg KS, & Bers DM (2012). Theoretical study of L-type Ca2+current inactivation kinetics during action potential repolarization and early afterdepolarizations. The Journal of Physiology 590: 4465-4481.

Mushlin PS, Cusack BJ, Boucek RJ, Andrejuk T, Li X, & Olson RD (1993). Time-related increases in cardiac concentrations of doxorubicinol could interact with doxorubicin to depress myocardial contractile function. British Journal of Pharmacology 110: 975-982.

O'Hara T, & Rudy Y (2011). Quantitative Comparison of Cardiac Ventricular Myocyte Electrophysiology and Response to Drugs in Human and Non-Human Species. American Journal of Physiology - Heart and Circulatory Physiology.

Octavia Y, Tocchetti CG, Gabrielson KL, Janssens S, Crijns HJ, & Moens AL (2012). Doxorubicin-induced cardiomyopathy: From molecular mechanisms to therapeutic strategies. Journal of Molecular and Cellular Cardiology 52: 1213-1225.

Olson HM, Young DM, Prieur DJ, LeRoy AF, & Reagan RL (1974). Electrolyte and Morphologic Alterations of Myocardium in Adriamycin-Treated Rabbits. The American Journal of Pathology 77: 439-454.

Olson RD, Gambliel HA, Vestal RE, Shadle SE, Charlier JHA, & Cusack BJ (2005). Doxorubicin cardiac dysfunction: effects on calcium regulatory proteins, sarcoplasmic reticulum, and triiiodothyronine. Cardiovascular Toxicology 5: 269-283.

Olson RD, & Mushlin PS (1990). Doxorubicin cardiotoxicity: analysis of prevailing hypotheses. The FASEB Journal 4: 3076-3086.

Olson RD, Mushlin PS, Brenner DE, Fleischer S, Cusack BJ, Chang BK, et al. (1988). Doxorubicin cardiotoxicity may be caused by its metabolite, doxorubicinol. Proceedings of the National Academy of Sciences 85: 3585-3589.

Qing T, Katz AM, & Kim DH (1991). Effects of azumolene on doxorubicin-induced Ca2+ release from skeletal and cardiac muscle sarcoplasmic reticulum. Biochimica et Biophysica Acta (BBA) - Molecular Cell Research 1094: 27-34.

Rees S, & Curtis MJ (1996). Which cardiac potassium channel subtype is the preferable target for suppression of ventricular arrhythmias? Pharmacology & Therapeutics 69: 199-217.

Sag CM, Köhler AC, Anderson ME, Backs J, & Maier LS (2011). CaMKII-dependent SR Ca leak contributes to doxorubicin-induced impaired Ca handling in isolated cardiac myocytes. Journal of Molecular and Cellular Cardiology 51: 749-759.

Sanguinetti MC, & Jurkiewicz NK (1990). Two components of cardiac delayed rectifier K+ current. Differential sensitivity to block by class III antiarrhythmic agents. The Journal of General Physiology 96: 195.

Serrano J, Palmeira CM, Kuehl DW, & Wallace KB (1999). Cardioselective and cumulative oxidation of mitochondrial DNA following subchronic doxorubicin administration1. Biochimica et Biophysica Acta (BBA) - Bioenergetics 1411: 201-205.

Shenasa H, Calderone A, Vermeulen M, Paradis P, Stephens H, Cardinal R, et al. (1990). Chronic doxorubicin induced cardiomyopathy in rabbits: mechanical, intracellular action potential, and adrenergic characteristics of the failing myocardium. Cardiovascular Research 24: 591-604.

Singal PK, Deally CMR, & Weinberg LE (1987). Subcellular effects of adryamicin in the heart: a concise review. Journal of Molecular and Cellular Cardiology 19: 817-828.

Suzuki T, Minamide S, Iwasaki T, Yamamoto H, & Kanda H (1997). Cardiotoxicity of a new anthracycline derivative (SM-5887) following intravenous administration to rabbits: comparative study with doxorubicin. Investigational new drugs 15: 219-225.

Szenczi O, Kemecsei P, Holthuijsen MFJ, van Riel NAW, van der Vusse GJ, Pacher P, et al. (2005). Poly(ADP-ribose) polymerase regulates myocardial calcium handling in doxorubicin-induced heart failure. Biochemical pharmacology 69: 725-732.

Takemura G, & Fujiwara H (2007). Doxorubicin-Induced Cardiomyopathy: From the Cardiotoxic Mechanisms to Management. Progress in Cardiovascular Diseases 49: 330-352.

ten Tusscher KH, & Panfilov AV (2006). Alternans and spiral breakup in a human ventricular tissue model. Am J Physiol Heart Circ Physiol 291: H1088-1100.

Terentyev D, Gyorke I, Belevych AE, Terentyeva R, Sridhar A, Nishijima Y, et al. (2008). Redox Modification of Ryanodine Receptors Contributes to Sarcoplasmic Reticulum Ca2+ Leak in Chronic Heart Failure. Circulation Research 103: 1466-1472.

Wang G-X, Wang Y-X, Zhou X-B, & Korth M (2001). Effects of doxorubicinol on excitation–contraction coupling in guinea pig ventricular myocytes. European Journal of Pharmacology 423: 99-107.

Wang YX, & Korth M (1995). Effects of doxorubicin on excitation-contraction coupling in guinea pig ventricular myocardium. Circulation research 76: 645-653.

Yeh ETH, Tong AT, Lenihan DJ, Yusuf SW, Swafford J, Champion C, et al. (2004). Cardiovascular complications of cancer therapy: diagnosis, pathogenesis, and management. Circulation 109: 3122-3131.

Table 1. Consensus % change values (α values) derived using method 1 and method 2 for all currents after exposure to DOX and DOXL.

	Method 1	Method 2			Data					
Current	**Average % Change**	**%Change 100/10µM**	**Mean IC_{50}/EC_{50}**	**IC_{50}/EC_{50} (µM)**	**% Change in Current Activity**	**Method**	**Dose**	**Time of Exposure**	**Temp**	**Reference**
Acute DOX										
	α	α								
I_{Rel}	+60%	+78%	29	13	Rat	+43%	Fractional release in %	10 µM	30min.	37°C	(Sag et al., 2011)
				0.125	R	+96%	Ca^{2+} release	10 µM	180min.	32°C	(Mushlin et al., 1993)
				75	Dog	+40%	Ca^{2+} release (nmol/mg)	50 µM	2min.	37°C	(Qing et al., 1991)
I_{Up}	-30%	-7%	1289	210	R	-30%	Ca^{2+} ATPase	90 µM	-	-	(Boucek et al., 1987b)
				2344	Dog	-23%	µM of Ca^{2+}/mg of protein/min	700µM	60min.	37°C	(Olson et al., 1988)
				967		-42%	µM of Pi/mg of protein/min	700µM	60min.	37°C	(Olson et al., 1988)
				1633		-30%	µM of Pi/mg of protein/min	700 µM	Every 30min.	37°C	(Boucek et al., 1987b)
I_{CaL}	+40%	+32%	217	58	R	+61%	Peak Ca^{2+} current (pA/pF)	90 µM	120min.	35-37°C	(Earm et al., 1994)
				376	GP	+21%	Peak Ca^{2+} current (pA/pF)	100 µM	60min.	35-36°C	(Wang & Korth, 1995)
I_{NaCa}	-40%	-6%	1581	4410	R	-2%	Peak NCX current (pA/pF)	90µM	60min.	35-37°C	(Earm et al., 1994)
				319		-22%	NCX exchange rate	90µM	-	-	(Boucek et al., 1987b)
				14	Dog	-85%	Ca^{2+} uptake on NCX exchanger	80µM	20 min.	37°C	(Caroni et al., 1981)
I_{NaK}	-20%	-1%	7251	106	Rat	-46%	µM of Pi /mg of protein/hr	90µM	30 min.	35°C	(Miwa et al., 1986)
				6300	R	-10%	µM of Pi /mg of protein/hr	700 µM	60 min.	37°C	(Olson et al., 1988)
				9300	Dog	-7%	µM of Pi /mg of protein/hr	700 µM	Every 30 min.	37°C	(Boucek et al., 1987b)
				13300		-5%	µM of Pi /mg of protein/hr	700 µM	60 min.	37°C	(Olson et al., 1988)
I_{Kr}	-40%	-44%	127	127	GP	-44%	I_k tail current (pA)	100 µM	60 min.	37°C	(Wang & Korth, 1995)

Chronic DOX											
I_{Rel}	-40%	-	-	-	R	-24%	mRNA	2 mg/kg	8 weeks (1)	NA	(Huang et al., 2003)
						-29%		1 mg/kg	8 weeks (2)	37°C	(Olson et al., 2005)
						-65%		2.5mg/kg	8 weeks (1)	30°C	(Arai et al., 1998)
I_{Up}	-10%	-	-	-	R	-26%	Ca^{2+} uptake (nmol/mg)	2.5mg/kg	8 weeks (1)	30°C	(Arai et al., 1998)
						-7%		1mg/kg	6-9 weeks (2)	30°C	(Dodd et al., 1993)
						-11%		1mg/kg	8 weeks (2)	32°C	(Olson et al., 2005)
I_{CaL}	+30%	-	-	-	Rat	+26%	Peak Ca^{2+} current (pA/pF)	2.5mg/kg	10 weeks (2)	22-25°C	(Keung et al., 1991)
I_{NaCa}	-20%	-	-	-	R	-13%	mRNA	2.5mg/kg	8 weeks (1)	30°C	(Arai et al., 1998)
						-25%	NCX exchanger	1 mg/kg	8 weeks (2)	NA	(Olson et al., 2005)
I_{NaK}	-20%	-	-	-	R	-15%	nM/mg	1 mg/kg	6-9 weeks (2)	37°C	(Dodd et al., 1993)
I_{Kr}	+50%	-	-	-	R	+50%	K^+ permeability	NA	NA	NA	(Shenasa et al., 1990)
Acute DOXL											
I_{Rel}	+0%	-	240	240	R	+4%	Ca^{2+} release	10µM	180min.	32°C	(Mushlin et al., 1993)
I_{Up}	-60%	-56%	8	8	Dog	-55%	Ca^{2+} loading in % of control	9µM	Every 30min.	25°C	(Boucek et al., 1987b)
I_{CaL}	-10%	-5%	190	190	GP	-5%	Peak Ca^{2+} current (nA)	10µM	15 min.	37°C	(Wang et al., 2001)
I_{NaCa}	-100%	-	-	-	R	-100%	NCX exchange rate	90µM	-	-	(Boucek et al., 1987b)
I_{NaK}	-50%	-50%	10	10	Dog	-50%	Na+/K+ ATPase in % of control	10µM	Every 30min.	37°C	(Boucek et al., 1987b)
I_{Kr}	+50%	+48%	11	11	GP	+48%	I_k tail current (pA)	10µM	15min.	37°C	(Wang et al., 2001)

Experimental observations (columns 6-10) and average estimates (α values in column 2) of changes in ion currents generated using method 1 for Na^+/K^+ pump (I_{NaK}), rapid delayed rectifying K^+ (I_{Kr}), SR Ca^{2+}-ATPase pump (I_{Up}), Na^+/Ca^{2+} exchanger (I_{NaCa}), the ryanodine receptor (I_{Rel}) and the L-type Ca^{2+} channel (I_{CaL}) after acute DOX, chronic DOX and acute DOXL exposure. Extrapolated values of IC_{50} and EC_{50} for each dose concentration after acute exposure to DOX and DOXL and their average value are also included (columns 4-5). From these IC_{50}/EC_{50} values, estimates of change in the currents after exposure to 100 µM of DOX and 10 µM of DOXL are calculated using method 2 (α values in column 3). Chronic DOX time of exposure is expressed in number of weeks that protocol was applied and the number of doses delivered each weak indicated in brackets. Abbreviations: Guinea Pig (GP), Rabbit (R), intracellular calcium concentration ($[Ca^{2+}]_i$), relaxation time (RT), APD at 90% repolarization (APD_{90}).

Table 2. Consensus values of % change derived using method 1 for APD, systolic Ca^{2+} concentration and Ca^{2+} relaxation time after exposure to DOX and DOXL.

	Method 1		Method 2		Data						
	Average % Change		Average IC_{50}/EC_{50}	IC_{50}/EC_{50} (μM)	Measurements of % Change	Description	Dose	Time of Exposure	Temp	Reference
Acute DOX										
APD	+50%		142	61	GP	+62%	APD_{90}	100μM	60min.	35-36°C	(Wang & Korth, 1995)
				223		+31%	APD_{90}	100μM	20min.	34-35°C	(Wang et al., 2001)
Ca^{2+}	**C**	+50%	92	92	GP	+52%	$[Ca^{2+}]_i$	100μM	60min.	35-36°C	(Wang & Korth, 1995)
	RT	+30%	233	233		+30%	$[Ca^{2+}]_i$ RT				(Wang & Korth, 1995)
	C	-40%	13	13	Rat	-43%	$[Ca^{2+}]_i$	10μM	15min.	37°C	(Sag et al., 2011)
Chronic DOX										
APD	-20%		-	-	R	-20%	APD_{90}	0.75mg/kg	6-9weeks (3)	37°C	(Shenasa et al., 1990)
					R	-23%	APD_{90}	1mg/kg	8 weeks (2)	32°C	(Doherty & Cobbe, 1990)
					R	+10%	APD_{90}	1.5mg/kg	6 weeks (2)	37°C	(Milberg et al., 2007)
Ca^{2+}	**C**	-55%	-	-	Rat	-	$[Ca^{2+}]_i$	2.5 mg/kg	8 weeks (1)	30°C	(Jensen, 1986)
						-55%	$[Ca^{2+}]_i$	2.5 mg/kg	2 weeks (3)	37°C	(De Angelis et al., 2010)
						+38%	$[Ca^{2+}]_i$	2 mg/kg	1 week (3)	30°C	(Kapelko et al., 1996)
						+74%	$[Ca^{2+}]_i$	2.5mg/kg	6 weeks (1)	37°C	(Szenczi et al., 2005)
	RT	+10%	-	-	Rat	+20%	$[Ca^{2+}]_i$ RT	2.5mg/kg	2 weeks (3)	37°C	(De Angelis et al., 2010)
						0%	$[Ca^{2+}]_i$ RT	2mg/kg	1 week (3)	30°C	(Kapelko et al., 1996)
Acute DOXL										
APD	-30%		30	30	GP	-25%	APD_{90}	10 μM	20 min.	34-35°C	(Wang et al., 2001)
Ca^{2+}	**C**	-20%	34	34	GP	-23%	$[Ca^{2+}]_i$	10 μM	15min.	34-35°C	(Wang et al., 2001)
	RT	+50%	92	92		+52%	$[Ca^{2+}]_i$ RT				(Wang et al., 2001)

Experimental observations (columns 5-9) for APD, Ca^{2+} concentration (Ca^{2+} C) and relaxation time (Ca^{2+} RT) after acute DOX, chronic DOX and acute DOXL exposure. Column 2 is the average % change estimates of changes derived using method 1. Column 3-4 are the extrapolated values of IC_{50} and EC_{50} for each dose concentration after acute exposure to DOX and DOXL and their average value generated using method 2. Chronic DOX time of exposure is expressed in number of weeks that protocol was applied and the number of doses delivered each weak indicated in brackets. Two large and opposite changes are reported for acute DOX effects on Ca^{2+} C, both values are reported as the consensus value and these different results are rationalized in the body text. Abbreviations: Guinea Pig (GP), Rabbit (R), intracellular calcium concentration ($[Ca^{2+}]_i$), relaxation time (RT), APD at 90% repolarization (APD_{90}).

Table 3. Model predictions of % change in APD, systolic Ca^{2+} concentration (Ca^{2+} C) and Ca^{2+} relaxation time (Ca^{2+} RT) before and after leak is increased.

	Acute 100 µM DOX			**Acute DOX**			**Chronic DOX**			**Acute DOXL**			**Acute 10 µM DOXL**		
	APD	Ca^{2+} C	Ca^{2+} RT	APD	Ca^{2+} C	Ca^{2+} RT	APD	Ca^{2+} C	Ca^{2+} RT	APD	Ca^{2+} C	Ca^{2+} RT	APD	Ca^{2+} C	Ca^{2+} RT
Rabbit	$\alpha = 1$														
	+18%	+84%	-6%	+4%	+174%	-1%	-14%	+87%	-13%	-28%	+11%	+44%	-27%	+23%	+37%
Human	$\alpha = 1$														
	+12%	+90%	+10%	+15%	+141%	+41%	-1%	+84%	+17%	-32%	-14%	+13%	-30%	+6%	+7%
Rabbit	$\alpha = 2$			$\alpha = 4$			$\alpha = 4$			$\alpha = 10$					
	+19%	+48%	+0%	+7%	+23%	+17%	-11%	-12%	+9%	-24%	-29%	+57%	-24%	-28%	+47%
Human	$\alpha = 2$			$\alpha = 2$			$\alpha = 3$			$\alpha = 2$					
	+11%	+13%	+20%	+13%	+47%	+58%	-7%	-38%	+3%	-38%	-38%	+18%	-37%	-26%	+13%
Consensus % Change	+50%	+50%	+30%	+50%	+50%	+30%	-20%	-55%	+10%	-30%	-20%	+50%	-30%	-20%	+50%

Predictions of % change for APD, systolic Ca^{2+} concentration (Ca^{2+} C) and Ca^{2+} relaxation time (Ca^{2+} RT) for acute DOX, chronic DOX, acute DOXL, acute 100 µM DOX and acute 10 µM DOXL exposures in rabbit and human models before leak is increased ($\alpha = 1$) and after leak is increased ($\alpha = 2, 3, 4, 10$) and comparison with consensus values for the average % change in APD, systolic Ca^{2+} concentration and Ca^{2+} relaxation time derived using method 1 (Table 2).

Table 4. Effects of currents on APD, Ca^{2+} concentration (Ca^{2+} C) and relaxation time (Ca^{2+} RT) calculated using factorial analysis.

	Acute 100 µM DOX		**Acute DOX**		**Chronic DOX**		**Acute DOXL**		**Acute 10 µM DOXL**	
APD	$\mathbf{I_{Kr}}$ $\mathbf{I_{CaL}}$	+6% +5%	$\mathbf{I_{Kr}}$ $\mathbf{I_{CaL}}$	+5% +7%	$\mathbf{I_{Kr}}$ $\mathbf{I_{CaL}}$ $\mathbf{I_{Leak}}$	-6% +5% -4%	$\mathbf{I_{Kr}}$ $\mathbf{I_{Up}}$ $\mathbf{I_{NaK}}$ $\mathbf{I_{Leak}}$	-7% -9% -15% -6%	$\mathbf{I_{Kr}}$ $\mathbf{I_{Up}}$ $\mathbf{I_{NaK}}$ $\mathbf{I_{Leak}}$	-7% -8% -14% -7%
Ca^{2+} C	$\mathbf{I_{CaL}}$ $\mathbf{I_{Leak}}$	+50% -72%	$\mathbf{I_{Up}}$ $\mathbf{I_{CaL}}$ $\mathbf{I_{NaCa}}$ $\mathbf{I_{Leak}}$	-81% +70% -67% -88%	$\mathbf{I_{CaL}}$ $\mathbf{I_{Leak}}$	+46% -109%	$\mathbf{I_{Up}}$ $\mathbf{I_{NaK}}$ $\mathbf{I_{Leak}}$	-113% +145 % -79%	$\mathbf{I_{Up}}$ $\mathbf{I_{NaK}}$ $\mathbf{I_{Leak}}$	-118% +161% -87%
Ca^{2+} RT	$\mathbf{I_{Leak}}$	+15%	$\mathbf{I_{Up}}$	+31%	$\mathbf{I_{NaCa}}$ $\mathbf{I_{Leak}}$	+9% +13%	$\mathbf{I_{Up}}$ $\mathbf{I_{NaK}}$ $\mathbf{I_{Leak}}$	+24% -13% -9%	$\mathbf{I_{Up}}$ $\mathbf{I_{NaK}}$ $\mathbf{I_{Leak}}$	+18% -13% +9%

Table 5: Sensitivity analysis testing model and data assumptions. In each case the derived default is the value from the main modelling reported in Results and consensus values derived from experiments (data shown in table 4).

Drug Model	Results from	Model	Change in APD	Change in Peak Ca^{2+}	Change in RT50
Acute DOX	Human model	Derived default	+13%	+47%	+58%
		0.5Hz	+10%	+131%	+12%
		I_{Kr} = -30%	+11%	+45%	+58%
		I_{Kr} = -20%	+10%	+43%	+57%
		I_{Kr} = -10%	+8%	+41%	+56%
		NCX = -10%	+13%	+17%	+23%
Acute DOX	Rabbit model	Derived default	+7%	+23%	+17%
		0.5Hz	+24%	+3%	+49%
		I_{Kr} = -30%	+4%	+23%	+17%
		I_{Kr} = -20%	+1%	+23%	+16%
		I_{Kr} = -10%	-1%	+23%	+16%
		NCX = -10%	+14%	+23%	+21%
Acute DOX	**Consensus values**		+50%	+50%	+30%
Chronic DOX	Human Model	Derived default	-6%	-49%	+6%
		0.5Hz	-4%	+5%	-19%
		I_{Kr} = +25%	-3%	-36%	+4%
		I_{Kr} = 0%	+0%	-35%	+7%
Chronic DOX	Rabbit Model	Derived default	-11%	-12%	+9%
		0.5Hz	+6%	-40%	+52%
		I_{Kr} = +25%	-6%	-8%	+9%
		I_{Kr} = 0%	-1%	-4%	+9%
Chronic DOX	**Consensus values**		-20%	-55%	+10%
Acute DOXL	Human Model	Derived default	-35%	-38%	+27%
		0.5Hz	-20%	+93%	-11%
Acute DOXL	Rabbit Model	Derived default	-24%	-29%	+57%
		0.5Hz	-12%	-45%	+122%
Acute DOXL	**Consensus values**		-30%	-20%	+50%
Acute 100 uM DOX	Human Model	Derived default	+11%	+13%	+20%
		0.5Hz	+9%	+4%	-20%
		I_{Kr} = -30%	+9%	+11%	+19%
		I_{Kr} = -20%	+8%	+9%	+19%
		I_{Kr} = -10%	+6%	+7%	+19%
		NCX = -10%	+11%	+18%	+20%
		I_{Ks}=-95%, I_{Kr} no effect	+71%	+102%	+43%
		I_{Ks}=-95%, I_{Kr} =-50%	+111%	+150%	+46%
Acute 100 uM DOX	Rabbit Model	Derived default	+19%	+48%	+0%
		0.5Hz	+31%	+33%	+11%
		I_{Kr} = -30%	+14%	+41%	+1%
		I_{Kr} = -20%	+11%	+37%	+1%
		I_{Kr} = -10%	+8%	+33%	+1%
		NCX = -10%	+18%	+51%	-1%
		I_{Ks}=-95%, I_{Kr} no effect	+12%	+40%	+0%
		I_{Ks}=-95%, I_{Kr} =-50%	+33%	+68%	-1%
Acute 100 uM DOX	**Consensus values**		+50%	+50%	+30%
Acute 10 uM DOXL	Human Model	Derived default	-37%	-26%	+2%
		0.5Hz	-19%	+104%	-15%
Acute 10 uM DOXL	Rabbit Model	Derived default	-24%	-28%	+47%
		0.5Hz	-6%	-44%	+105%
Acute 10 uM DOXL	**Consensus values**		-30%	-20%	+50%

Figure 1. Rabbit and human models: changes in APD and Ca^{2+} concentration for acute DOX, chronic DOX, acute DOXL, acute 100 μM DOX and acute 10 μM DOXL before (red dashed line) and after leak increase (blue dash-dotted line) with respect to the corresponding control model with no drug effects (black solid line).

Figure 2. Simulated caffeine exposure in the human model. The red dashed line shows the predicted I_{NaCa} current following a simulated caffeine exposure with no change in I_{NaCa} but with inhibition of I_{NaK} by 50%. The black line shows the simulated I_{NaCa} current following a simulated caffeine exposure using the reference model.

Figure 3. Effect of currents on APD, systolic Ca^{2+} concentration and Ca^{2+} relaxation time for (left) acute DOX model derived at 100 μM (centre) acute DOX, chronic DOX and acute DOXL models obtained at a range of experimental dosages and (right) acute DOXL model derived at 10 μM.

Figure 4. Comparison between rabbit and human models. Panels A-E show results with no change in SR leak and panels F-J show results after SR leak is optimised for changes in APD, Ca^{2+} concentration (Ca^{2+} C) and Ca^{2+} relaxation time (Ca^{2+} RT) for acute DOX, chronic DOX, acute DOXL, acute 100 μM DOX and acute 10 μM DOXL.

OPEN ACCESS

KING'S College LONDON

King's Research Portal

Link to publication record in King's Research Portal

Citation for published version (APA):
Niederer, S. A., Curtis, M. J., & Fernandez-Chas, M. (2017). Mechanism of doxorubicin cardiotoxicity evaluated by integrating multiple molecular effects into a biophysical model. British Journal of Pharmacology.

Citing this paper
Please note that where the full-text provided on King's Research Portal is the Author Accepted Manuscript or Post-Print version this may differ from the final Published version. If citing, it is advised that you check and use the publisher's definitive version for pagination, volume/issue, and date of publication details. And where the final published version is provided on the Research Portal, if citing you are again advised to check the publisher's website for any subsequent corrections.

General rights
Copyright and moral rights for the publications made accessible in the Research Portal are retained by the authors and/or other copyright owners and it is a condition of accessing publications that users recognize and abide by the legal requirements associated with these rights.

•Users may download and print one copy of any publication from the Research Portal for the purpose of private study or research.
•You may not further distribute the material or use it for any profit-making activity or commercial gain
•You may freely distribute the URL identifying the publication in the Research Portal

Take down policy
If you believe that this document breaches copyright please contact librarypure@kcl.ac.uk providing details, and we will remove access to the work immediately and investigate your claim.

Download date: 19. Jul. 2018

Drug Effects with No SR Leak Included

A. Acute DOX

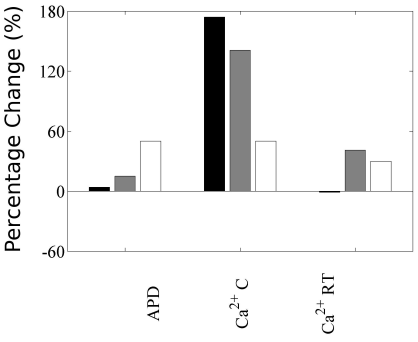

B. Chronic DOX

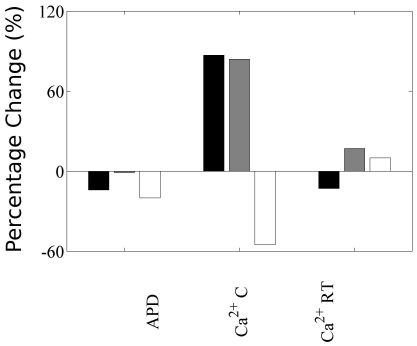

C. Acute DOXL

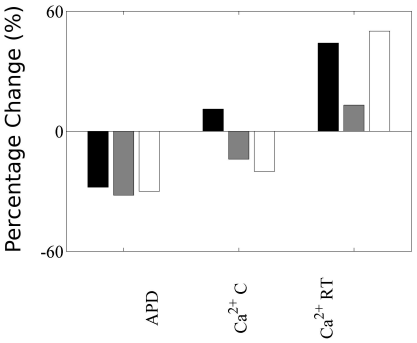

D. Acute 100 µM DOX

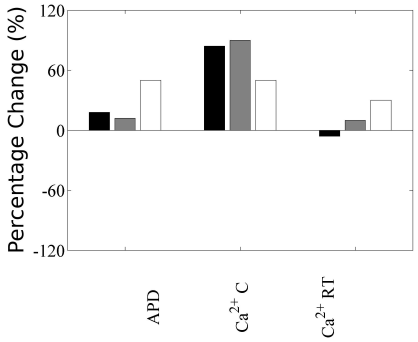

E. Acute 10 µM DOXL

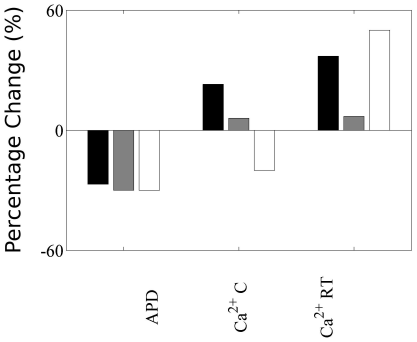

Drug Effects with SR Leak Included

F. Acute DOX

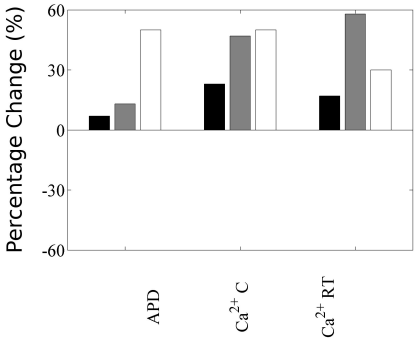

G. Chronic DOX

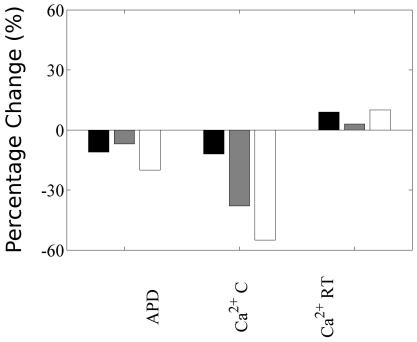

H. Acute DOXL

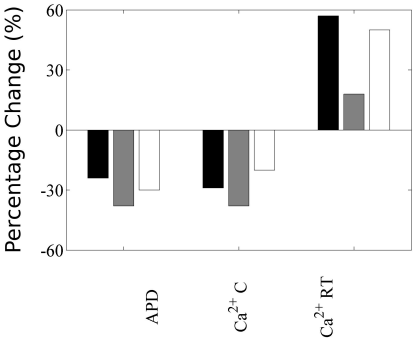

I. Acute 100 µM DOX

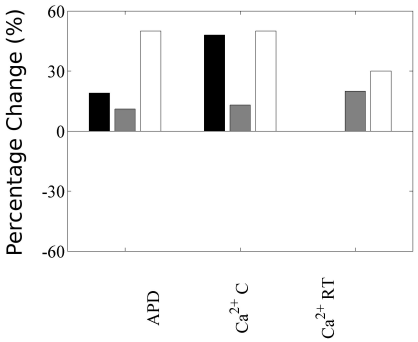

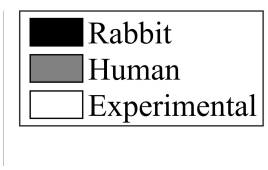

J. Acute 10 µM DOXL

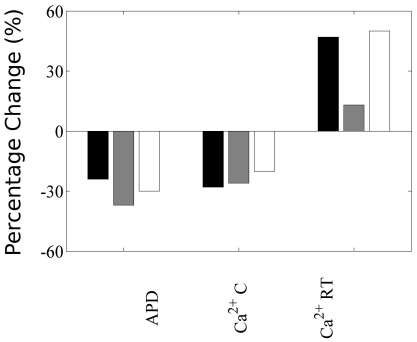

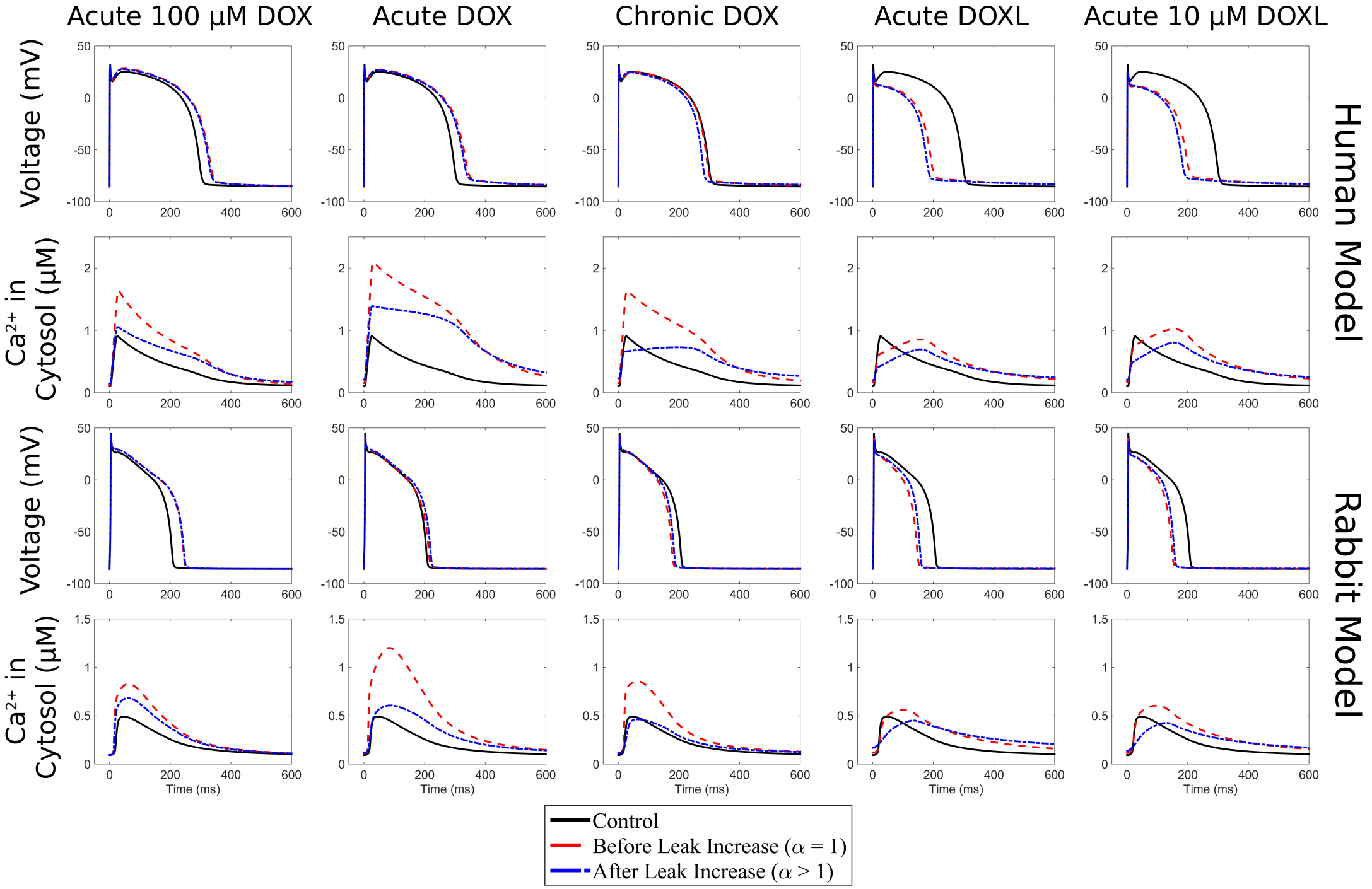
Acute 100 μM DOX
Acute DOX
Chronic DOX
Acute DOXL
Acute 10 μM DOXL
Human Model
Rabbit Model
Voltage (mV)
Ca2+ in Cytosol (μM)
Time (ms)
Control
Before Leak Increase (α = 1)
After Leak Increase (α > 1)

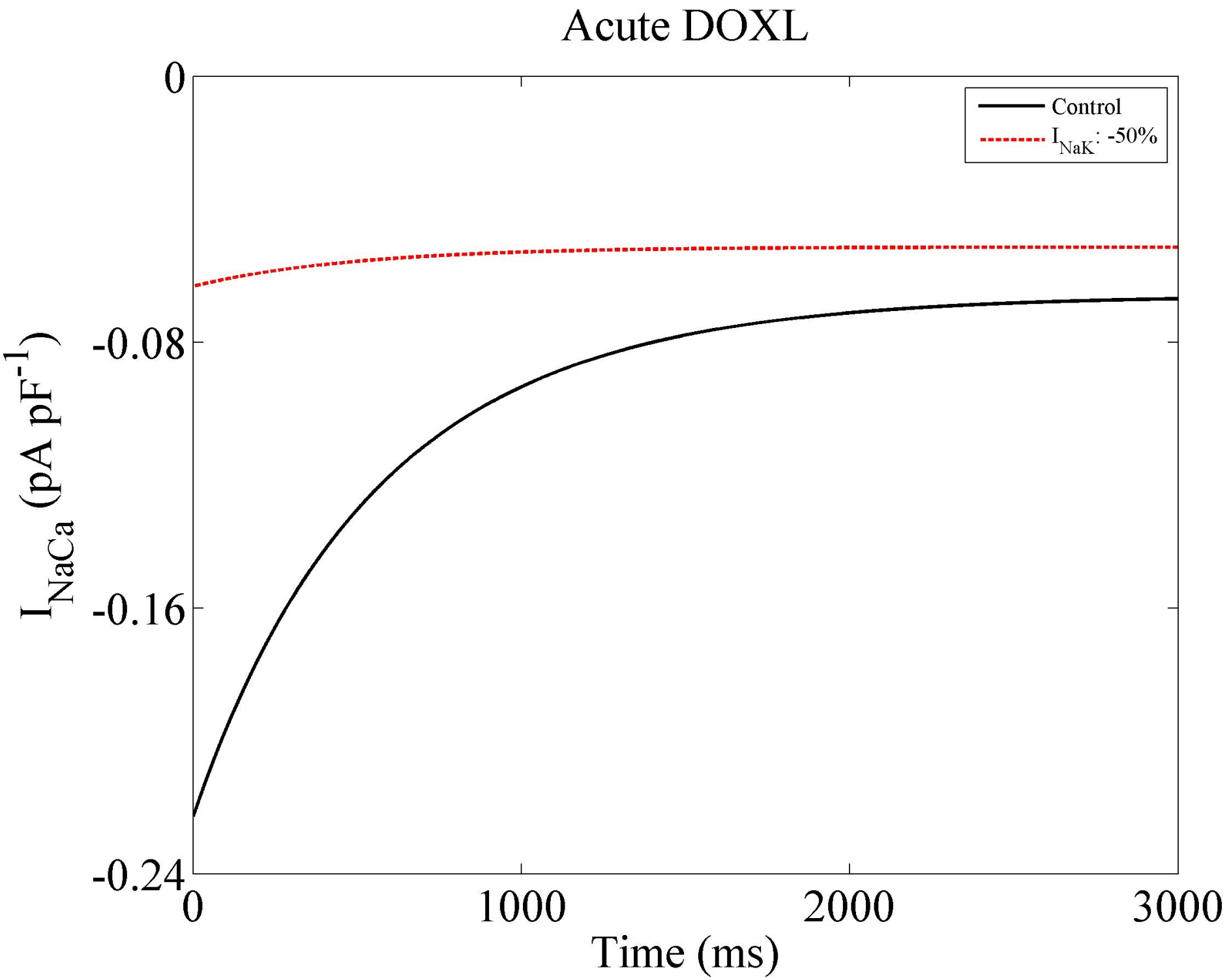
Acute DOXL
Control
I_{NaK}: -50%
0
-0.08
-0.16
-0.24
I_{NaCa} (pA pF^{-1})
0
1000
2000
3000
Time (ms)

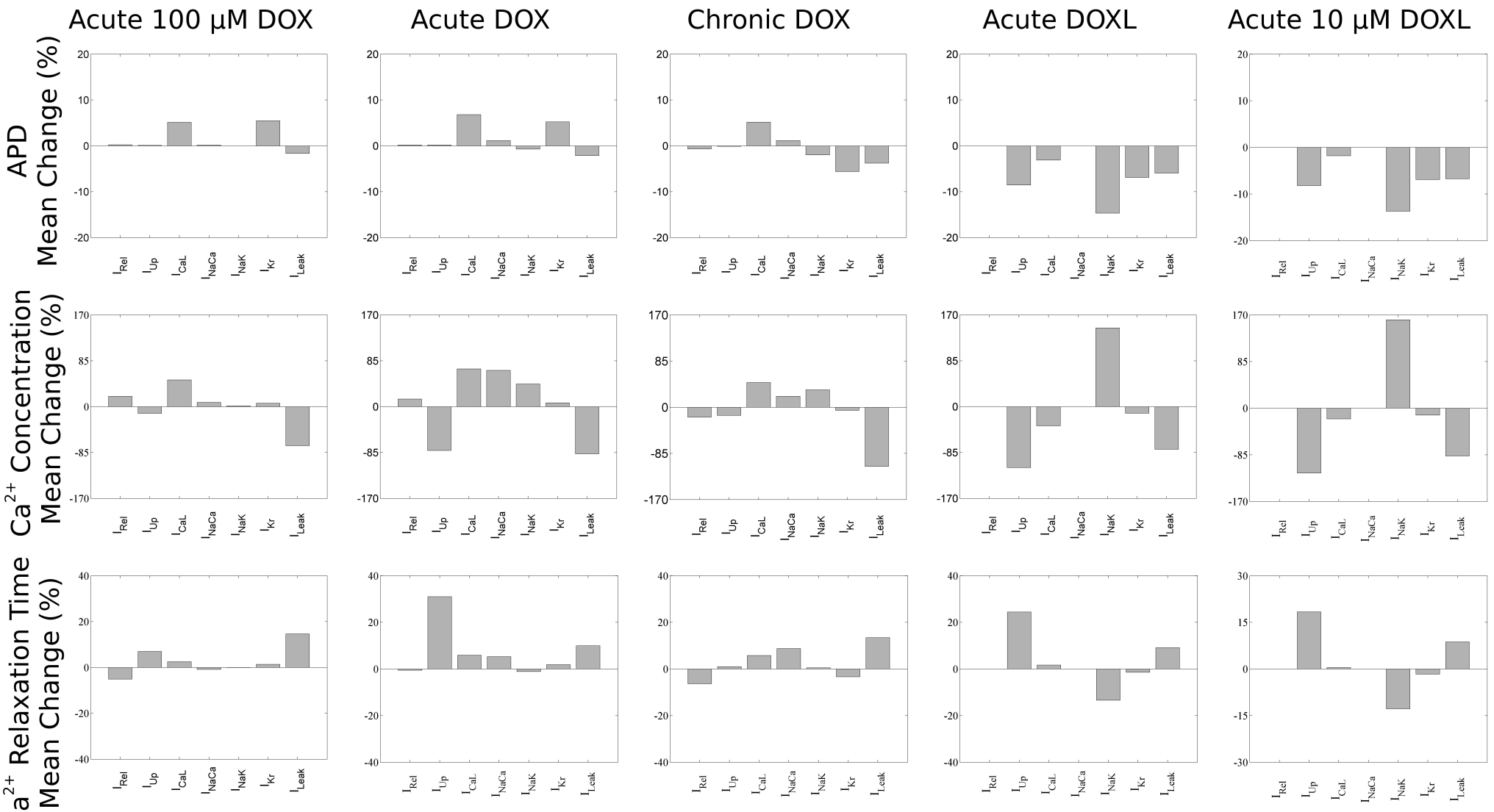
Acute 100 µM DOX
Acute DOX
Chronic DOX
Acute DOXL
Acute 10 µM DOXL
APD
Mean Change (%)
Ca2+ Concentration
Mean Change (%)
Ca2+ Relaxation Time
Mean Change (%)
IRel
IUp
ICaL
INaCa
INaK
IKr
ILeak